Available online at www.sciencedirect.com
SCIENCE DIRECT®
Journal of Solid State Chemistry 177 (2004) 1405–1411
JOURNAL OF SOLID STATE CHEMISTRY
http://elsevier.com/locate/jssc

Crystal growth, structure determination and magnetism of a new $m = 3$, $n = 1$ member of the $A_{3n+3m}A'_nB_{3m+n}O_{9m+6n}$ family of oxides: 12R-$Ba_{12}Rh_{9.25}Ir_{1.75}O_{33}$

Katharine E. Stitzer,[a] Ahmed El Abed,[b,1] Jacques Darriet,[b,2] and Hans-Conrad zur Loye[a,*]

[a] *Department of Chemistry and Biochemistry, University of South Carolina, 631 Sumter St., Columbia, SC 29208, USA*
[b] *Institut de Chimie de la Matière Condensée de Bordeaux (ICMCB-CNRS), 87 Avenue du Dr. Schweitzer, 33608 Pessac Cedex, France*

Received 27 August 2003; received in revised form 4 November 2003; accepted 23 November 2003

Abstract

Single crystals of a new Ba–Rh–Ir–O oxide were grown from a molten potassium carbonate flux. The new compound, $Ba_{12}Rh_{9.25}Ir_{1.75}O_{33}$, is structurally related to the 2H-hexagonal perovskite structure and contains pseudo one-dimensional chains of alternating units of ten face-sharing $(Rh/Ir)O_6$ octahedra and one $(Rh/Ir)O_6$ trigonal prism. The magnetic susceptibility of $Ba_{12}Rh_{9.25}Ir_{1.75}O_{33}$ is featureless, indicating the absence of magnetic order. The oxide is a semiconductor with a room temperature resistance of 280 Ω.

Keywords: 2H-perovskite related structure; Crystal growth; Magnetism

1. Introduction

There continues to be much interest in the preparation and investigation of a family of oxides ($A_{3n+3m}A'_nB_{3m+n}O_{9m+6n}$) structurally related to the 2H-hexagonal perovskite [1–4]. This interest is spurred on by both the compositional flexibility of this family of oxides, as almost every element from the periodic chart has been inserted into these structures, as well as by the structural variety exhibited by these phases. Recently, the development of successful crystal growth approaches for many of these new compounds has enabled the structure determination of many compositions [1,4–6], which in turn has provided important structural insights into these oxides.

As shown by Darriet and Subramanian [7] and more recently by Darriet et al. [8] the structures of these oxides can all be described as resulting from the hexagonal stacking of $m[A_3O_9]$ layers and $n[A_3A'O_6]$ layers, followed by the subsequent filling of the interstitial octahedral sites. The general formula that can be derived from the stacking of such layers is $A_{3n+3m}A'_nB_{3m+n}O_{9m+6n}$, where n and m are integers and the cation A is an alkaline earth metal while cations A' and B can be any number of metals including alkali, alkaline earth, transition, main group, or rare earth metals. The structures are characterized by one-dimensional chains of face-sharing $A'O_6$ trigonal prisms and BO_6 octahedra along the c-axis of the hexagonal unit cell.

An equivalent expression for this family of oxides is $A_{1+x}(A'_xB_{1-x})O_3$ where the composition variable $x = n/(3m + 2n)$ and can be envisaged to be any number between 0 and 1/2 [9]. Thus a value of $x = 0$ corresponds to the $BaNiO_3$ structure [10] while a value of $x = 1/2$ corresponds to the Sr_4PtO_6 structure [11], i.e. the two end members of this family of oxides. The compounds can also be described as modulated composite structures, where the structure is depicted as two mutually interacting subsystems modulated along z but periodic in the xy plane [8,9,12–14].

Numerous examples of the $n = 1$, $m = 0$ $(x = 1/2)$ member of the 2H-perovskite related family have been

*Corresponding author. Fax: +8037778508.
E-mail address: zurloye@sc.edu (H.-C. zur Loye).
[1] Permanent address: Mohamed I Univ., Facultédes Sciences, Oujda, Morocco.
[2] Also for correspondence.

0022-4596/$ - see front matter © 2003 Elsevier Inc. All rights reserved.
doi:10.1016/j.jssc.2003.11.021

synthesized including Sr_4PtO_6 [11], Sr_3NaSbO_6 [15], Ca_3NiMnO_6 [16], Sr_3NiPtO_6 [17], Ca_3NiIrO_6 [18], Ca_3CuRhO_6 [3], Sr_3ScNiO_6 [19], Sr_3NiPbO_6 [20], Sr_3NiRhO_6 [21], and Ca_3CuIrO_6 [22]. In addition, an ever increasing number of examples of other structures, including $Sr_6Rh_5O_{15}$ ($n=1$, $m=1$) [23,24], $Ba_8CoRh_6O_{21}$ ($n=3$, $m=5$) [25], $Ba_9Rh_8O_{24}$ ($n=1$, $m=2$) [26], $Sr_4CuIr_2O_9$ ($n=3$, $m=1$) [27], and $Ba_5PdMn_3O_{12}$ ($n=3$, $m=2$) [28] have been prepared as both powders and in single-crystal form.

There are, surprisingly, very few examples of oxides belonging to this family that contain two precious metals in the polyhedral chains [29]. In an attempt to prepare a new mixed Rh/Ir oxide of this family, both iridium and rhodium, together with barium carbonate, were dissolved in a potassium carbonate flux. A single-phase product of $Ba_{12}Rh_{9.25}Ir_{1.75}O_{33}$ was isolated and structurally characterized. The structure and magnetic property of this new oxide are discussed within.

2. Experimental

2.1. Crystal growth

For $Ba_{12}Rh_{9.25}Ir_{1.75}O_{33}$, Rh powder (0.1029 g, 1.0 mmol; Engelhard, 99.5%), Ir powder (0.1923 g, 1.0 mmol; Engelhard, 99.5%), $BaCO_3$ (0.5920 g, 3.0 mmol; Alfa, 99.95%) and K_2CO_3 (17.75 g, 128 mmol; Fisher, reagent grade) were mixed thoroughly and placed in an alumina crucible. The filled crucible was covered and heated in air from room temperature to the reaction temperature of 1150°C at 600°C/h, held at 1150°C for 72 h, and then slowly cooled to 800°C at 15°C/h. The reaction was then cooled to room temperature by turning off the furnace. The flux was removed with water, aided by the use of sonication, and the crystals were isolated manually.

2.2. Magnetic susceptibility

The magnetic susceptibility of $Ba_{12}Rh_{9.25}Ir_{1.75}O_{33}$ was measured using a Quantum Design MPMS XL SQUID magnetometer. For magnetic measurements, loose single crystals of $Ba_{12}Rh_{9.25}Ir_{1.75}O_{33}$ were placed into a gelatin capsule, which was placed inside a plastic straw. Samples were measured under both field cooled (fc) and zero field cooled (zfc) conditions. In either case, the magnetization was measured in the temperature range of 2–300 K. Susceptibility measurements were carried out in applied fields of 1, 5, and 20 kG. The very small diamagnetic contribution of the gelatin capsule containing the sample had a negligible contribution to the overall magnetization, which was dominated by the sample.

2.3. Data collection

Several single crystals of $Ba_{12}Rh_{9.25}Ir_{1.75}O_{33}$ were tested and the quality of the diffraction data (crystal quality) was assessed on the basis of the size and sharpness of the diffraction spots. The data collection was carried out on Enraf-Nonius Kappa CCD diffractometer using Mo$K\alpha$ radiation ($\lambda = 0.71069$ Å). Data processing and the refinement were performed using the JANA2000 program package [30]. An analytical absorption correction was applied, for which the shape of the crystal was determined using the video microscope of the Kappa CCD instrument. A rapid scan on the CCD diffractometer gave a rhombohedral cell with lattice parameters of $a = 10.0492(2)$ Å and $c = 28.386(3)$ Å. Final data were collected using this cell and the structure solved by a combination of direct methods and difference Fourier syntheses, and refined by full-matrix least-squares against F^2, using JANA2000. Relevant crystallographic information is compiled in Table 1, and the atomic coordinates for $Ba_{12}Rh_{9.25}Ir_{1.75}O_{33}$ are presented in Table 2.

2.4. Electrical conductivity measurement

The electrical resistivity was measured on a non-oriented single crystal in the 65–300 K range using the 4-point probe method in a standard cryostat.

3. Results and discussion

3.1. Structures

Black hexagonal plates of $Ba_{12}Rh_{9.25}Ir_{1.75}O_{33}$ were grown and isolated from a carbonate melt containing Ba–Ir–Rh–O. The plates were, on average, 0.1–0.4 mm in the largest dimension. The growth of these crystals further contributes to the mounting evidence that high temperature carbonate solutions are particularly amenable for the growth of rhodium-containing single crystals and, as evidenced by these results, for mixed rhodium/iridium crystals as well. $Ba_{12}Rh_{9.25}Ir_{1.75}O_{33}$ represents the first mixed Rh/Ir metal oxide belonging to this structural family and is a rare example of a mixed platinum group metal oxide belonging this family [29].

$Ba_{12}Rh_{9.25}Ir_{1.75}O_{33}$ is a $m=3$, $n=1$ member of the $A_{3n+3m}A'_nB_{3m+n}O_{9m+6n}$ family of oxides (A = Ba, A' = Rh/Ir, B = Rh/Ir) and is formed by the stacking of three repeats of $3\times[Ba_3O_9]$ layers followed by $1\times[Ba_3(Rh/Ir)O_6]$ layer and is therefore a 12R layer structure. An approximate [110] view of $Ba_{12}Rh_{9.25}Ir_{1.75}O_{33}$ is shown in Fig. 1. The structure consists of a repeat of 10 octahedra followed by one trigonal prism. Using the alternative composite structure description, $A_{1+x}(A'_xB_{1-x})O_3$, we can re-write the composition as

Table 1
Crystal data and structure refinement for $Ba_{12}Rh_{9.25}Ir_{1.75}O_{33}$

Empirical formula	$Ba_{12}Rh_{9.25}Ir_{1.75}O_{33}$	
Formula weight	3464.16 g/mol	
Temperature	293 K	
Wavelength	Mo$K\alpha$ ($\lambda = 0.71069$ Å)	
Crystal system	Trigonal	
Space group	$R32$	
Unit-cell dimensions	$a = 10.0492(2)$ Å	$\alpha = 90°$
	$b = 10.0492(2)$ Å	$\beta = 90°$
	$c = 28.386(3)$ Å	$\gamma = 120°$
Volume	2482.51(2) Å^3	
Z	3	
Density (calculated)	6.815 g/cm^3	
Crystal size	$0.09 \times 0.09 \times 0.05$ mm^3	
$h\,k\,l$ range	$-16 \leqslant h \leqslant 11,\ -12 \leqslant k \leqslant 16,\ -45 \leqslant l \leqslant 45$	
θ_{max}	35°	
Linear absorption coeff	19.43 mm^{-1}	
Absorption correction	Gaussian	
T_{min}/T_{max}	0.160/0.378	
No of reflections	16538	
R_{int}	0.0590	
No of independent reflections	2344	
Criterion for observed reflections	$I > 3.0\sigma(I)$	
Number observed reflections	1670	
$F(000)$	4461	
Goodness-of-fit on F^2	1.46	
R factors (observed)	R(F) = 0.0244 wR(F^2) = 0.0529	
R factors (all)	R(F) = 0.0417 wR(F^2) = 0.0590	
No. of refined parameters	99	
Weighting scheme	$w = 1/(\sigma^2(I) + 0.00004I^2)$	
Diff. Fourier residues	[−3.08, +2.60] e/Å^3	

Table 2
Atomic coordinates and equivalent isotropic displacement parameters (Å^2) for $Ba_{12}Rh_{9.25}Ir_{1.75}O_{33}$

Atom	Wyckoff position	Occupancy	x	y	z	U_{eq} (Å^2)
Rh1/Ir1	6c	72%/28%	0	0	0.09545(3)	0.0195(3)
Rh2/Ir2	6c	86%/14%	0	0	0.27944(3)	0.0075(2)
Rh3/Ir3	6c	88%/12%	0	0	0.45614(3)	0.0058(2)
Rh4/Ir4	6c	86%/14%	0	0	0.63190(2)	0.0077(3)
Rh5/Ir5	6c	85%/15%	0	0	0.81048(3)	0.0091(2)
Rh6/Ir6	6c	45%/5%	0	0	0.00659(9)	0.0121(7)
Ba1	9d	100%	0.34839(7)	0	0	0.0121(2)
Ba2	9e	100%	0.32605(7)	0	1/2	0.0161(3)
Ba3	18f	100%	0.00321(5)	−0.34303(6)	0.08340(2)	0.0134(2)
O1a	18f	41%	−0.1668(13)	−0.1043(13)	0.0479(4)	0.034(3)
O1b	18f	59%	−0.1215(10)	−0.1603(9)	0.0521(3)	0.034(3)
O2	18f	100%	0.1497(7)	0.1538(6)	0.1460(2)	0.036(3)
O3	18f	100%	−0.1558(6)	−0.1573(7)	0.23588(19)	0.019(2)
O4	18f	100%	0.1589(6)	0.1548(6)	0.3232(2)	0.010(2)
O5	18f	100%	−0.1565(7)	−0.1583(7)	0.41337(15)	0.009(2)
O6	9e	100%	−0.1617(7)	0	1/2	0.009(2)

$Ba_{1.0909}(Rh/Ir)O_3$, where $x = 1/11$ (0.0909) and the modulation $\gamma = (1+B)/2 = 6/11$. (Since rhodium and iridium are disordered over all sites, it is not possible to assign separate A' and B occupancies.) The structure is one of only a few commensurate examples of this family that are known and that do not belong to the $n = 1$, $m = 0$ group.

The structure of $Ba_{12}Rh_{9.25}Ir_{1.75}O_{33}$ is closely related to that of $Ba_{12}Co_{11}O_{33}$, which was first observed by TEM [31] and subsequently fully characterized by single-crystal X-ray diffraction [32]. This oxide also consists of chains of 10 octahedra followed by one trigonal prism, however, it crystallizes with orthorhombic rather than rhombohedral symmetry. $Ba_{12}Co_{11}O_{33}$ is

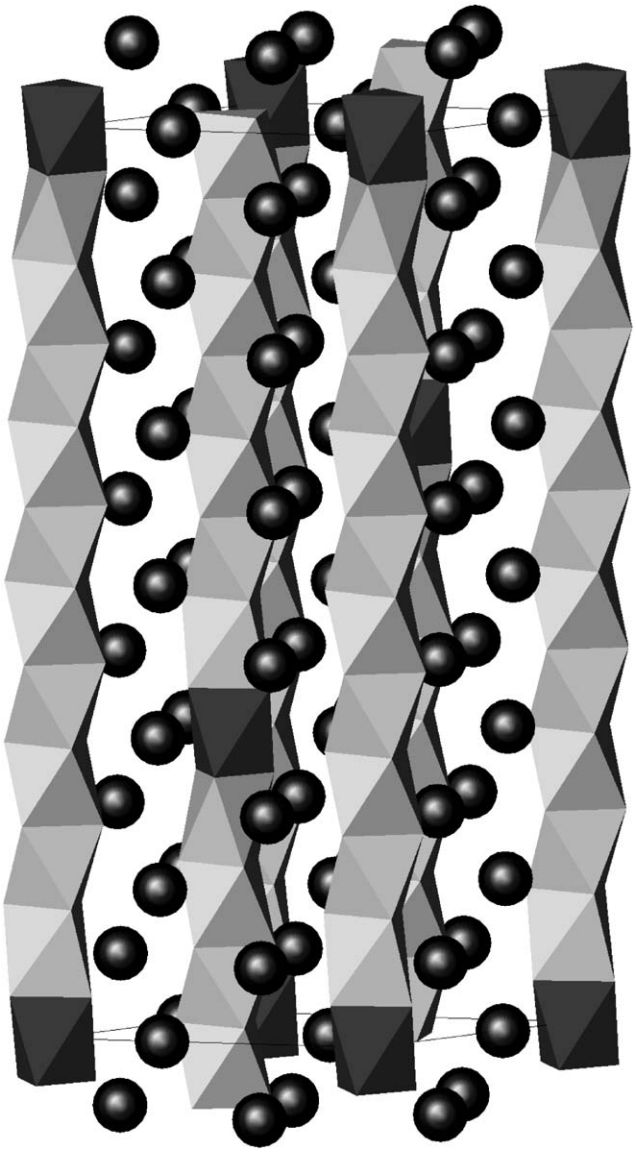

Fig. 1. Approximate [110] view of the structure of $Ba_{12}Rh_{9.25}Ir_{1.75}O_{33}$ consisting of chains of 10 face-sharing $(Rh/Ir)O_6$ octahedra followed by one $(Rh/Ir)O_6$ "trigonal prism". Dark gray: $(Rh/Ir)O_6$ "trigonal prism"; light gray: $(Rh/Ir)O_6$ octahedra; black spheres: Ba cations.

a member of the closely related $A_{4m+4n}A'_nB_{4m+2n}O_{12m+9m}$ family of oxides, where m/n is the ratio of $[A_8O_{24}]$ and $[A_8A'_2O_{18}]$ layers in the sequence. As with the rhombohedral series, the layer stacking is hexagonal and the general formula can also be expressed as $A_{1+x}(A'_xB_{1-x})O_3$, however the layers involved are different ($[A_8O_{24}]$ and $[A_8A'_2O_{18}]$ vs. $[A_3O_9]$ and $[A_3A'O_6]$ layers). It is important to note that, nonetheless, by this formalism, both $Ba_{12}Co_{11}O_{33}$ and $Ba_{12}Rh_{9.25}Ir_{1.75}O_{33}$ are $x = 1/11$ members of $A_{1+x}(A'_xB_{1-x})O_3$, making $Ba_{12}Rh_{9.25}Ir_{1.75}O_{33}$ only the second example of an oxide structure with $x = 1/11$ to have been synthesized and structurally characterized.

During the structure solution of $Ba_{12}Rh_{9.25}Ir_{1.75}O_{33}$, it was noted that if the oxygen position, O1, is fully occupied, the isotropic thermal parameter was quite large ($\sim 10\,Å^2$). A Fourier difference plot around this position clearly indicated that this position is split creating a second position O1b close to that of O1a. Due to this splitting and the fact that the z-position of the two oxygen positions is not identical, the position of Rh6(Ir6) (trigonal prism) is very slightly shifted from its true position of (0,0,0) along the z-axis to (0,0,0.00659(9))—see Table 2. There are, consequently, two Rh6–Rh1 distances (2.522 and 2.897 Å). Depending on the occupancy of the atoms, i.e. O1a and O1b, there are two deformed coordination environments of Rh6(Ir6). When the O1a position is occupied, the environment of Rh6(Ir6) most closely resembles that of a distorted octahedron, while when the O1b position is occupied, the environment of Rh6(Ir6) more closely resembles that of a distorted trigonal prism. Furthermore, regardless of whether O1a or O1b is occupied, the coordination environment of Rh1(Ir1), the nearest neighbor to Rh6(Ir6), is that of a deformed octahedron; however, the octahedron is less distorted when O1b is occupied than when O1a is occupied.

The structure of the chain of ten octahedra followed by one trigonal prism, Fig. 1, is more distorted than expected. In particular, the trigonal prismatic site is highly distorted; and depending on the occupation of the oxygen (O1a or O1b), the site may more closely resembles a distorted trigonal prism (O1a) or a distorted octahedron (O1b). Iridium and rhodium are located on both "trigonal prismatic" and octahedral sites. Selected interatomic distances are located in Table 3; the M–O distances are consistent with others reported in literature [23,27]. The M–M distances range from 2.49 Å in the middle of the sequence to 2.90 Å for distances between the "trigonal prism" and its nearest neighbor octahedron, giving rise to a V-shaped Rh(Ir)–Rh(Ir) distance vs. chain-position plot as shown in Fig. 2. This phenomenon is not unique to $Ba_{12}Rh_{9.25}Ir_{1.75}O_{33}$, as it has been observed for $Sr_6Rh_5O_{15}$ [23], $Ba_9Rh_8O_{24}$ [26], $Ba_{12}Co_{11}O_{33}$ [31] $Ba_{11}Rh_{10}O_{30}$ and $Ba_{32}Rh_{29}O_{87}$ [33], although it is most pronounced for structures having long sequences of face-sharing octahedra.

The modulation of $\gamma = 6/11$ yields a c_1 parameter of $c/11 = 2.58$ Å for the $[Rh/Ir]O_3$ chain, a c_2 parameter of $c/6 = 4.73$ Å for the [Ba] chain, and an average layer height of 2.366 Å for the overall structure. An idealized octahedron height of 2.366 Å ($c/12 = 28.386/12 = 2.366$ Å) is "shorter" than one might expect for an Rh/IrO_6 octahedron and is, in fact, not what is observed. The structure is quite distorted and in addition to the $M-M$ distance giving rise to a V-shaped plot due to a shift off the ideal cation positions, the oxygens are also quite shifted generating "taller" octahedra than the ideal structure would produce.

Table 3
Selected interatomic distances (Å) for $Ba_{12}Rh_{9.25}Ir_{1.75}O_{33}$

Atom–atom	Distance (Å)		Atom–atom	Distance (Å)	
Rh1(Ir1)–O2	2.094(5)	(×3)	Ba1–O4	2.826(7)	(×4)
Rh1(Ir1)–O1a	1.993(13)	(×3)	Ba1–O1a	2.592(14)	(×2)
Rh1(Ir1)–O1b	1.906(10)	(×3)	Ba1–O1b	2.579(10)	(×2)
Rh2(Ir2)–O4	2.008(5)	(×3)	Ba1–O5	2.837(5)	(×2)
Rh2(Ir2)–O3	2.001(7)	(×3)	Ba2–O2	2.934(8)	(×2)
Rh3(Ir3)–O6	2.047(6)	(×3)	Ba2–O6	2.838(7)	(×2)
Rh3(Ir3)–O5	1.994(7)	(×3)	Ba2–O3	2.674(6)	(×2)
Rh4(Ir4)–O4	2.027(7)	(×3)	Ba2–O5	2.987(6)	(×2)
Rh4(Ir4)–O5	2.038(7)	(×3)	Ba3–O2	2.629(7)	(×1)
Rh5(Ir5)–O2	1.964(7)	(×3)	Ba3–O4	2.716(5)	(×1)
Rh5(Ir5)–O3	2.051(7)	(×3)	Ba3–O6	2.880(4)	(×1)
Rh6(Ir6)–O1a	1.877(13)	(×3)	Ba3–O1a	2.671(16)	(×1)
Rh6(Ir6)–O1a	2.131(13)	(×3)	Ba3–O1b	2.835(11)	(×1)
Rh6(Ir6)–O1b	1.946(9)	(×3)	Ba3–O3	2.864(7)	(×1)
Rh6(Ir6)–O1b	2.212(9)	(×3)	Ba3–O3	2.943(8)	(×1)
Rh1(Ir1)–Rh5(Ir5)	2.670(1)	(×1)	Ba3–O5	2.808(9)	(×1)
Rh1(Ir1)–Rh6(Ir6)	2.522(3)	(×1)	Ba3–O5	2.860(9)	(×1)
Rh1(Ir1)–Rh6(Ir6)	2.897(3)	(×1)			
Rh2(Ir2)–Rh4(Ir4)	2.517(1)	(×1)			
Rh2(Ir2)–Rh5(Ir5)	2.553(1)	(×1)			
Rh3(Ir3)–Rh3(Ir3)	2.490(1)	(×1)			
Rh3(Ir3)–Rh4(Ir4)	2.499(1)	(×1)			

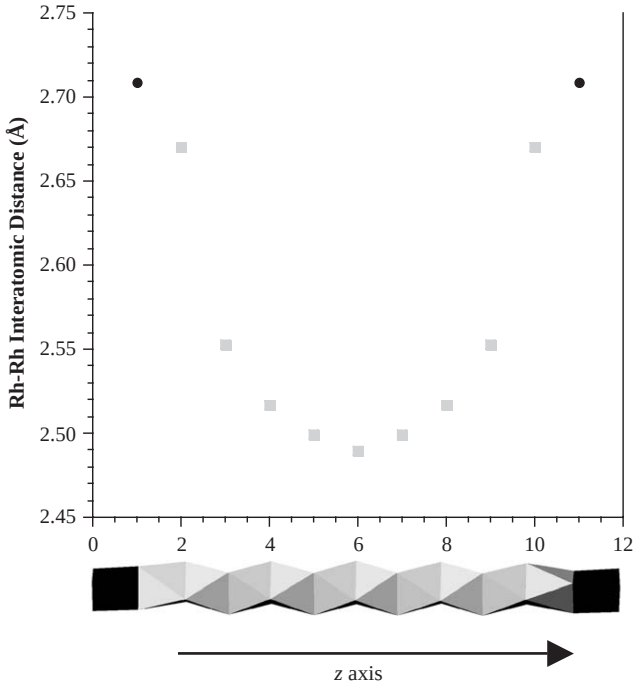

Fig. 2. Plot of the Rh(Ir)–Rh(Ir) interatomic distance as a function of placement within the polyhedral chain for $Ba_{12}Rh_{9.75}Ir_{1.75}O_{33}$ where (●) is the distance between a Rh(Ir) in a "trigonal prism" and a Rh(Ir) in an adjacent octahedron and (■) is the distance between a Rh(Ir) in an octahedron to a Rh(Ir) in an adjacent octahedron.

We believe that this "accordion effect" of the Rh(Ir)–Rh(Ir) distances within the polyhedral chains represents a structural relaxation of the trigonal prismatic height, caused by the unsustainable 2:1 height ratio between trigonal prisms and octahedra that result from the idealized stacking of $[AO_3]$ and $[A_3A'BO_6]$ layers [33] to achieve a more reasonable octahedron height. This has been observed in other structural members of this family where the trigonal prism is not of ideal height in comparison to the octahedra (2:1) but rather where this height ratio has decreased at the expense of the trigonal prism to a ratio of at most 1.6–1.7. In fact even this reduced ratio is only achieved in structures such as Ba_4PtO_6 and Sr_4PtO_6, which have a repeat of one trigonal prism to one octahedron; in structures with longer octahedral sequences this ratio decreases further and levels out at a value of only ~1.1. As a result, the trigonal prism is much smaller than expected, almost matching the size of the octahedra, which in turn have increased in height. In $Ba_{12}Rh_{9.25}Ir_{1.75}O_{33}$ the height of the "inner" octahedra have increased to an average value of 2.512 Å versus an ideal value of 2.366 Å, while the trigonal prisms has shrunk to a value of 2.958 Å versus an ideal value of 4.73 Å (2 × 2.366 Å) yielding a reduced trigonal prism to octahedron height ratio of 1.18. This is shown in Fig. 3, where the polyhedral height as a function of position along the chain for $Ba_{12}Rh_{9.25}Ir_{1.75}O_{33}$ is plotted. It appears that this height expansion starts in the middle of the chain and creates this accordion effect that causes a compression of the trigonal prism. The result, of course, is a chemically more reasonable Rh/IrO_6 octahedron size. We believe that this octahedral expansion—trigonal prismatic compression, is a general phenomena for this family of oxides.

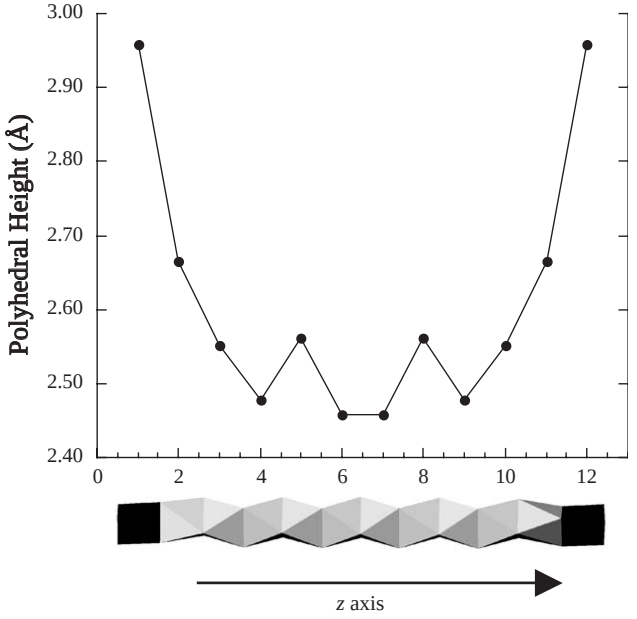

Fig. 3. Plot of the polyhedral height as a function of placement within the polyhedral chain for $Ba_{12}Rh_{9.75}Ir_{1.75}O_{33}$.

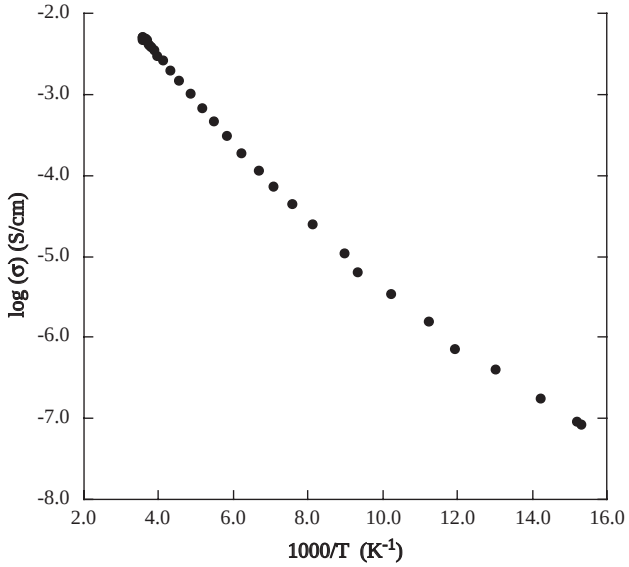

Fig. 4. Temperature dependence of the electrical conductivity measured using a non-oriented single crystal of $Ba_{12}Rh_{9.25}Ir_{1.75}O_{33}$.

3.2. Conductivity

Conductivity measurements were carried out on a non-oriented single crystal of $Ba_{12}Rh_{9.25}Ir_{1.75}O_{33}$ and the temperature dependence of the conductivity is shown in Fig. 4. The data are not perfectly linear over the entire temperature range, but clearly indicate that the material behaves like a semiconductor. The room temperature resistance of the crystal was 280 Ω.

3.3. Magnetism

The magnetic susceptibility of $Ba_{12}Rh_{9.25}Ir_{1.75}O_{33}$ was investigated using loose single crystals. The temperature dependence of the magnetic susceptibility is shown in Fig. 5. No magnetic transitions are apparent in the data down to the lowest measured temperature of 2 K. Furthermore, the zfc and fc data overlay at all temperatures. Fitting all of the susceptibility data to a modified Curie–Weiss law that includes a term for the temperature independent paramagnetism (TIP) according to the following equation:

$$\chi = \frac{C}{T-\theta} + \mathrm{TIP}$$

yields a Curie constant of 0.147 emu K/mol with $\mu_{\mathrm{eff}} = 1.08\,\mu_B$, $\theta = -1$ K, TIP = 0.0011 emu/mol. By charge balance, one might propose an oxidation state scheme of 2 Rh(III), 7.25 Rh(IV) and 1.75 Ir(IV). Such a scheme would yield a theoretical spin only moment of 5.18 μ_B, which is considerably higher than the measured moment. We can suggest two reasons for this low

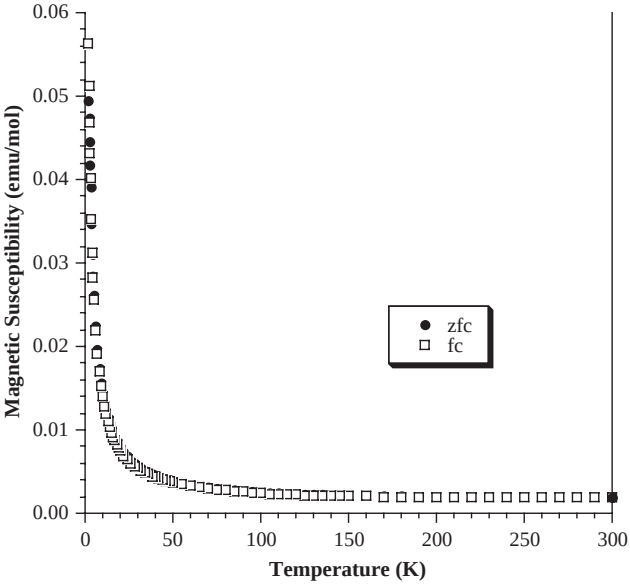

Fig. 5. Temperature dependence of the zero field cooled (zfc; ●) and field cooled (fc; □) magnetic susceptibility of loose single crystals of $Ba_{12}Rh_{9.25}Ir_{1.75}O_{33}$ in an applied field of 5 kG.

magnetic moment: (1) we expect spin orbit coupling to reduce the magnetic moment of iridium (IV) and rhodium (IV) and (2), we expect the presence of very strong exchange interactions between the metals in the chain, particularly between metals located in the middle of the chain away from the trigonal prisms, to cause an additional reduction of the magnetic moment. We should point out that this low moment is not unusual for these oxide materials and has been observed in several other materials [23].

To explain the Curie-like behavior at low temperatures we need to consider the coupling between the spins. Rh(III) is diamagnetic and, hence, will break any magnetic interactions along a given chain. This will create short magnetic clusters within the chains that are separated by Rh(III) cations; within these short magnetic clusters, the number of magnetic cations (Rh(IV) $s = 1/2$, Ir(IV) $s = 1/2$) can be even or odd. For antiferromagnetic interactions, an even number of $s = 1/2$ cations will produce an $S = 0$ ground state. Assuming that the magnetic interactions are strong, this will lead to a large temperature range over which these segments will contribute essentially nothing to the magnetic moment. An odd number of magnetic $s = 1/2$ cations, on the other hand, will lead to an $S = 1/2$ ground state. Such $S = 1/2$ segments will obey the Curie law at low temperatures, where the temperature range over which the $S = 1/2$ Curie law behavior is observed will depend on the strength of the antiferromagnetic interactions. This will hold true for trimers, pentamers, heptamers, etc. In $Ba_{12}Rh_{9.25}Ir_{1.75}O_{33}$ there will be a statistical distribution of even and odd clusters contributing to the overall magnetic moment. The even clusters can be neglected due to the strong exchange interactions and only the odd clusters need to be considered. Here we expect a statistical size distribution where the strong exchange interactions within these clusters will lead to Curie-like behavior over a large temperature range, as is experimentally observed.

4. Conclusion

In summary, a new rhodium/iridium-containing oxide, structurally related to the 2H-hexagonal perovskite structure, was grown from a molten carbonate flux. The structure of $Ba_{12}Rh_{9.25}Ir_{1.75}O_{33}$ consists of repeats of alternating face-sharing octahedra and trigonal prisms and has a very long sequence of 10 face-sharing $(Rh,Ir)O_6$ octahedra followed by one $(Rh,Ir)O_6$ trigonal prism. $Ba_{12}Rh_{9.25}Ir_{1.75}O_{33}$ represents a rare example of a mixed platinum group metal oxide of this family.

Acknowledgments

Financial support from the National Science Foundation through Grant DMR: 0134156 is gratefully acknowledged. Further details of the crystal structure investigations can be obtained from the Fachinformationszentrum Karlsruhe, 76344 Eggenstein-Leopoldshafen, Germany (fax: +49-7247-808-666; mailto: crysdata @fiz.karlsruhe.ed) on quoting the depository number CSD-413346 for $Ba_{12}Rh_{9.25}Ir_{1.75}O_{33}$.

References

[1] K.E. Stitzer, J. Darriet, H.-C. zur Loye, Curr. Opin. Solid State Mater. Sci. 5 (2001) 535.
[2] A. El Abed, E. Gaudin, J. Darriet, Acta Crystallogr. C 58 (2002) i138.
[3] M.J. Davis, M.D. Smith, H.-C. zur Loye, J. Solid State Chem. 173 (2003) 122.
[4] A. El Abed, E. Gaudin, H.-C. zur Loye, J. Darriet, Solid State Sci. 5 (2003) 59.
[5] M.J. Davis, M.D. Smith, K.E. Stitzer, H.-C. zur Loye, J. Alloys Compd. 351 (2003) 95.
[6] A. El Abed, S.E. Elqebbaj, M. Zakhour, M. Champeaux, J.M. Perez-Mato, J. Darriet, J. Solid State Chem. 161 (2001) 300.
[7] J. Darriet, M.A. Subramanian, J. Mater. Chem. 5 (1995) 543.
[8] J.M. Perez-Mato, M. Zakhour-Nakhl, F. Weill, J. Darriet, J. Mater. Chem. 9 (1999) 2795.
[9] M. Evain, F. Boucher, O. Gourdon, V. Petricek, M. Dusek, P. Bezdicka, Chem. Mater. 10 (1998) 3068.
[10] J.J. Lander, Acta Crystallogr. 4 (1951) 148.
[11] J.J. Randall, L. Katz, Acta Crystallogr. 12 (1959) 519.
[12] K. Ukei, A. Yamamoto, Y. Watanabe, T. Shishido, T. Fukuda, Acta Crystallogr. B 49 (1993) 67.
[13] M. Zakhour-Nakhl, J.B. Claridge, J. Darriet, F. Weill, H.-C. zur Loye, J.M. Perez-Mato, J. Am. Chem. Soc. 122 (2000) 1618.
[14] M. Zakhour-Nakhl, F. Weill, J. Darriet, J.M. Perez-Mato, Int. J. Inorg. Mater. 2 (2000) 71.
[15] P.D. Battle, S.J. Hartwell, C.A. Moore, Inorg. Chem. 40 (2001) 1716.
[16] G.V. Bazuev, V.G. Zubkov, I.F. Berger, T.I. Arbuzova, Solid State Sci. 1 (1999) 365.
[17] T.N. Nguyen, D.M. Giaquinta, H.-C. zur Loye, Chem. Mater. 6 (1994) 1642.
[18] J.B. Claridge, R.C. Layland, R.D. Adams, H.-C. zur Loye, Z. Anorg. Allg. Chem. 623 (1997) 1131.
[19] M. James, J.P. Attfield, Chem. Eur. J. 2 (1996) 737.
[20] M.D. Smith, J.K. Stalick, H.-C. zur Loye, Chem. Mater. 11 (1999) 2984.
[21] K.E. Stitzer, W.H. Henley, J.B. Claridge, H.-C. zur Loye, R.C. Layland, J. Solid State Chem. 164 (2002) 220.
[22] A. Tomaszewska, Hk. Müller-Buschbaum, Z. Anorg. Allg. Chem. 619 (1993) 534.
[23] K.E. Stitzer, A. El Abed, J. Darriet, H.-C. zur Loye, J. Am. Chem. Soc. 123 (2001) 8790.
[24] J.B. Claridge, H.-C. zur Loye, Chem. Mater. 10 (1998) 2320.
[25] H.-C. zur Loye, K.E. Stitzer, M.D. Smith, A. El Abed, J. Darriet, Inorg. Chem. 40 (2001) 5152.
[26] K.E. Stitzer, M.D. Smith, J. Darriet, H.-C. zur Loye, Chem. Commun. (2001) 1680.
[27] P.D. Battle, G.R. Blake, J. Sloan, J.F. Vente, J. Solid State Chem. 136 (1998) 103.
[28] P.D. Battle, J.C. Burley, E.J. Cussen, J. Darriet, F. Weill, J. Mater. Chem. 9 (1999) 479.
[29] J.C. Burley, P.D. Battle, N.A. Jordan, J. Sloan, F. Weill, J. Solid State Chem. 174 (2003) 96.
[30] V. Petricek, M. Dusek, JANA2000: Programs for Modulated and Composite Crystals, Institute of Physics, Praha, Czeck Republic, 2000.
[31] K. Boulahya, M. Parras, J.M. Gonzalez-Calbet, Chem. Mater. 12 (2000) 2727.
[32] J. Darriet, L. Elcoro, A. El Abed, E. Gaudin, J.M. Perez-Mato, Chem. Mater. 14 (2002) 3349.
[33] K.E. Stitzer, A. El Abed, J. Darriet, H.-C. zur Loye, J. Am. Chem. Soc., 2004, in press.